ELSEVIER

Journal of Volcanology and Geothermal Research 65 (1995) 297–317

Journal of volcanology and geothermal research

Simulations of magma ascent and pyroclast dispersal at Vulcano (Aeolian Islands, Italy)

Silvia Coniglio, Flavio Dobran

Global Volcanic and Environmental Systems Simulation, Via Caio Mario 27, 00192 Rome, Italy

(Received 25 August 1993; revised and accepted 1 July 1994)

Abstract

Two-phase flow models of magma ascent in volcanic conduits and pyroclast dispersal in the pressure- and temperature-stratified atmosphere were employed to study the consistency of the Palizzi pumice fall eruption phase and the last eruption of Vulcano with modeling predictions. The input data for magma ascent modeling were constrained by the limited availability of petrological, volcanological and geophysical data, and consisted of magma composition, crystal content, conduit geometry, and pressure and temperature of magma in the magma chamber. The magma ascent model was used to establish the locations of magma exsolution and fragmentation levels, gas and pyroclast velocities, pressure, and pyroclast volumetric fractions at the exits of conduits of different diameters and lengths. The vent exit conditions of gas and pyroclasts corresponding to different magma compositions and conduit geometry were employed in the pyroclastic dispersion modeling to establish the distribution of gas and pyroclasts in the atmosphere and along the slopes of the volcano during the first few minutes of the eruptions in order to determine the volcanic column and flow behavior along the slopes of the volcano. The results from simulations showed that the Palizzi pumice fall eruption phase and the last eruption of Vulcano which produced bread-crust bombs are consistent with magma ascent and pyroclastic dispersion models. Using the available volcanological, petrological and geophysical data as well as the modeling results, an eruptive scenario of each cycle of Vulcano was hypothesized where the chemical characteristics of new magma supply into the volcanic system and magma remaining in the system after preceding eruptions, mechanical characteristics of the magma ascent pathways, and the conditions of aquifers surrounding these pathways determine the duration of phreatic, phreatomagmatic, magmatic, and lava flow activities within each cycle. The modeling results also suggested that the Palizzi pumice fall eruption phase ejected magma with a dissolved water content of about 2 wt.% from a vent diameter of about 30 m, and that the dissolved water content in magma during the last eruption of Vulcano ranged between 1 and 2 wt.%. Detailed modeling of various eruptive phases and adequate volcanic hazard assessment at Vulcano not only requires the development of magma–water interaction and hydrothermal circulation models, but also the collection of modeling oriented volcanological, petrological, and geophysical data.

1. Introduction

Recent modeling of magma ascent along volcanic conduits (Dobran, 1992; Papale and Dobran, 1993, 1994) and dispersion of pyroclasts above volcanic vents (Wohletz et al., 1984; Valentine and Wohletz, 1989; Valentine et al., 1991; Dobran et al., 1993; Giordano and Dobran, 1994; Neri and Dobran, 1994) allows for better constraints on the volcanic eruption parameters obtained from volcanological, petrological, geophysical and observational data. Modeling of magma ascent from a magma chamber to the Earth's surface which allows for changing magma composition

SSDI 0377-0273(94)00048-4

along the conduit due to gas exsolution, and for flow regime changes from bubbly flow below the magma fragmentation level to the particle/droplet flow above this level where the pyroclasts are dispersed in the continuous gas phase, permits an accurate determination of vent exit conditions. Pressure, temperature, gas and pyroclast velocities, and pyroclast size and volumetric fraction at the exit of a volcanic vent are the required data for input into a pyroclastic dispersion model of volcanic columns. The magma ascent and pyroclastic dispersion models thus provide powerful tools not only to constrain the available volcanological, petrological and geophysical data associated with different eruptive events, but also to study these events when such data are lacking.

Vulcano is an active volcanic island in the Aeolian Archipelago (southern Tyrrhenian Sea). The volcanic activity of Vulcano can be associated with the collision between the European and African plates (Gasparini et al., 1982) with different stages of activity forming different structures on the island (Keller, 1980; Frazzetta et al., 1983; Frazzetta and La Volpe, 1987). The present cone La Fossa is nested in La Fossa Caldera with its volcanic activity starting about 14,000 years ago. During the subsequent stages of evolution, Vulcano exhibited magmatic, phreatomagmatic and lava flow activities. In particular, the end of the first phase of the Palizzi cycle about 2,200 years ago ended with a magmatic eruption which produced a pumice fall deposit. Each eruption cycle of La Fossa is characterized by a progressive decrease in the degree of magma–water interaction. The last eruption of Vulcano lasted from 1888 to 1890, and since 1980 Vulcano has displayed increasing fumarolic activity and gas temperatures which produced an increase in the monitoring activity of the volcano to the present day (Martini et al., 1980; Barberi et al., 1991).

The physical modeling approach of studying the possible volcanic processes at Vulcano should be considered as a major tool for the quantification of future volcanic hazard, since the island of Vulcano is very small and even a small-scale volcanic event could be catastrophic to the island's inhabitants and tourists (Barberi et al., 1991). The phreatic and phreatomagmatic eruptions of Vulcano constitute the major eruption events of this volcano and should be studied by the appropriate physical models which involve magma–water interaction. The magmatic eruptions of Vulcano occurred during the Palizzi and other cycles of this volcano after phreatomagmatic eruptions which produced wet- and dry-surges and flows. These eruptions are useful for constraining the volcanological, petrological and geophysical data with the magma ascent and pyroclastic dispersion models where magma–water interaction is not considered, as well as for establishing possible conditions of magma in conduits before and after the phreatomagmatic events, such as during the Palizzi's and last eruption cycles of Vulcano. The results from such a modeling approach show that the Palizzi pumice fall eruption and last eruption of Vulcano which produced bread-crust bombs are consistent with modeling, and that they can be used to establish an eruptive scenario of each cycle of Vulcano.

2. Geological Setting of the Island of Vulcano

Vulcano is the most southerly of the seven volcanic islands in the Aeolian Archipelago (Fig. 1). Its evolution has been influenced by NW–SE and NE–SW regional tectonic trends (Ghisetti, 1979; Fabbri et al., 1980; Gabbianelli et al., 1991). Keller (1980), Frazzetta et al. (1983) and Frazzetta and La Volpe (1987) recognized six stages of evolution of the island, starting with Vulcano Primordiale and continuing with Piano Caldera, Lentia Complex, La Fossa Caldera, La Fossa Cone, and Vulcanello. The eruptive magmas have evolved with time from the calcalkaline to shoshonitic suites, the latter being represented especially by the products of La Fossa Cone. All the explosive and effusive products of La Fossa Cone show their shoshonitic affinity with a high potassium content and have a chemical composition ranging from trachytic to the more evolved rhyolitic.

La Fossa Cone was formed in the middle of La Fossa Caldera $14{,}000 \pm 6{,}000$ years ago by the Punta Roia lavas (Frazzetta et al., 1983, 1984). The main products of La Fossa activity are dry and wet surges, pyroclastic flows, fall deposits, and minor lava flows (Frazzetta and La Volpe, 1987). The volcanic sequence described by Keller (1980) was interpreted by Frazzetta et al. (1983) in terms of six volcanic cycles: Punte Nere, nonidentified, Palizzi, Commenda, Pietre Cotte, and Modern. The last eruption or Modern cycle at La Fossa took place from 1888 to 1890 and was well described by Mercalli and Silvestri (1891) who were eyewit-

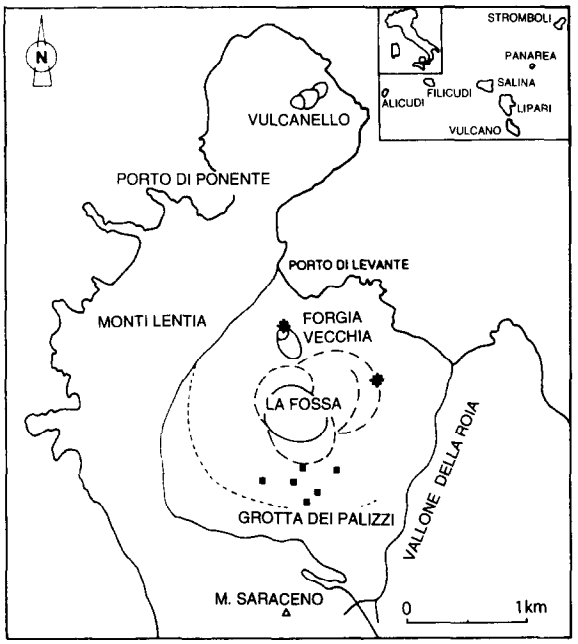

Fig. 1. Location map showing the island of Vulcano and the area of La Fossa Cone. Solid squares represent outcrop locations of the Palizzi cycle including the pumice fall deposits. Stars represent outcrop locations of the 1888–1890 cycle including the bread-crust bombs. The circles represent craters corresponding to different cycles (see text), with the full circle indicating the present crater (after Frazzetta and La Volpe, 1983).

nesses during this eruption and who coined the term "Vulcanian" for the spectacular explosions produced by the opening of the obstructed conduit. Since 1890, Vulcano has been producing fumarolic activity with variable intensities.

The Punte Nere cycle (from 14,000–6,000 years ago) produced dry-surge and fall deposits, and ended with the effusion of the Punte Nere lava flows of trachytic composition. The Palizzi cycle (pumice fall about 2,200 and lava flow about 1,600 years ago) is divided into two phases. The first phase of the cycle began with the emplacement of wet- and dry-surges and ended with a pumice fall, whereas the second phase began with wet- and dry-surges and ended with a trachytic lava flow. The Commenda cycle (AD 729) opened with an explosion breccia of trachytic composition that locally grades to a pyroclastic flow, followed with wet- and dry-surges, and ended with an obsidian lava flow. The Pietre Cotte cycle (1739) opened with wet- and dry- surges, continued with pumice fall, and ended with obsidian lava flow. The last eruption (1888–1890) involved explosion breccia, dry-surges, ash-falls, and ejection of bread-crust bombs primarily of rhyolitic composition.

2.1. Characteristics of the Palizzi Pumice Fall

The present outcrops of the Palizzi pumice deposit are scattered along the southern slope of La Fossa Cone (Fig. 1). The pumice beds are essentially of fall origin because they lack a matrix and are normally graded where they lie on level topography (Frazzetta et al., 1983). This deposit reaches a maximum thickness of 2 m at the break-in-slope of the volcano. The pumice fragments range in size from several centimeters to about 30 cm, with a mean value of about 10 cm. The glass matrix of the pumice fragments has a trachytic composition. The crystal phases consist principally of sanidine, plagioclase and clinopyroxene, and scarce amounts of dark amphibole and mica. The chemical composition of pumice obtained by Keller (1980) is shown in Table 1. The pumice fall and the underlying phreatomagmatic flow deposits are undisturbed and do not show evidence of erosion at their top surfaces.

2.2. Characteristics of the 1888–1890 eruption deposits

The last eruption of Vulcano produced surge, fall and flow deposits which are represented by the lapilli-and-block and coarse-and-fine beds around the crater rim. The bread-crust bombs lie on various slopes of the volcano, some of which are shown in Fig. 1. The bombs

Table 1
Anhydrous compositions of erupting magmas at Vulcano recalculated to 100%. Sample V227 from the Palizzi pumice phase (Keller, 1980), and average values of 12 bread-crust bomb samples (table 2, De Fino et al., 1991)

Composition	SiO_2	TiO_2	Al_2O_3	Fe_2O_3	FeO	MnO	MgO	CaO	Na_2O	K_2O
Palizzi	60.43	0.73	18.14	2.38	2.80	0.07	1.35	2.80	4.25	7.05
1888–1890	71.10	0.24	14.53	2.67	–	0.09	0.23	0.89	3.63	6.62

are characterized by an aphyric glassy matrix of rhyolitic composition and xenoliths of trachytic composition with a maximum abundance of 8 vol.% (De Fino et al., 1991). The composition of the glassy matrix of bombs (De Fino et al., 1991) is summarized in Table 1.

3. Summary of magma ascent and pyroclastic dispersion models

3.1. Magma ascent modeling and input data for simulations

Dobran (1992) and Papale and Dobran (1993, 1994) developed a nonequilibrium two-phase flow model for magma ascent in volcanic conduits. This model describes a quasi steady-state and one-dimensional flow of magma from the magma chamber to the surface (Fig. 2), where the flow of magma is assumed to be isothermal and where no account is taken of heat and mass transfer across the conduit wall. As the magma ascends and decompresses along a conduit, it begins to exsolve at a height z_s above the magma chamber. Above z_s, the gas bubbles grow by exsolution of dissolved gas and decompression. Eventually, a critical

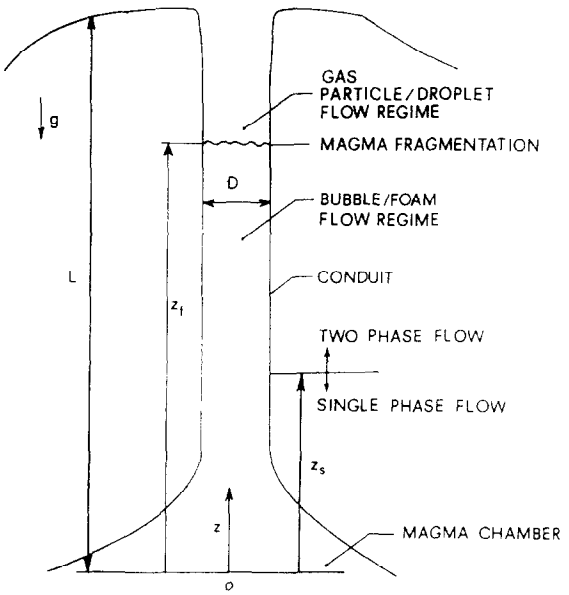

Fig. 2. Illustration of a volcanic conduit of length L and constant diameter D. Magma is accelerated from the magma chamber o at $z=0$, begins exsolving water at a height z_s, and fragments at a height z_f above the magma chamber.

packing density is reached at which further bubble growth is prevented by the magma viscosity and neighboring bubbles. When this occurs, the bubbly flow regime cannot be maintained anymore and the magma fragments at a height z_f above the magma chamber. For purely magmatic eruptions, this critical bubble packing appears to be well defined by the critical gas volumetric fraction $\alpha=0.75$ (Sparks, 1978; Dobran, 1992). Above z_f, the flow in the conduit is governed by a two-phase gas-particle/droplet flow where the fragmented magma particles/drops (or pyroclasts) are entrained in a continuous gas phase. Assuming a conduit with a constant diameter, the maximum mass flow-rate is realized when the flow becomes critical or choked at the conduit exit. When choking occurs, the conditions above the vent cannot influence magma flow characteristics along the conduit. The thermal equilibrium assumption between magma and gas is justified by the very large thermal capacity of magma, short flow transit time through the conduit, and absence of magma–water interaction (Wilson et al., 1980; Wilson and Head, 1981; Dobran, 1992). In contrast, mechanical nonequilibrium effects may be very important in the upper region of a conduit where gas and pyroclasts velocities are different due to the different acceleration characteristics of these phases in the presence of high flow gradients (Dobran, 1992).

The two-phase flow conditions in the conduit were modeled by solving numerically the conservation of mass and balance of momentum equations (of gas and magma below the magma fragmentation level and gas and pyroclasts above this level), together with the constitutive equations for gas exsolution, magma density and viscosity, and interfacial drag between gas and pyroclasts and between the gas-magma mixture and conduit wall (Dobran, 1992). Following Papale and Dobran (1993), it was assumed that water is the only gas phase, that chemical equilibrium exists between exsolved and dissolved water, and that the liquid magma can be described by the regular solution theory (Ghiorso et al., 1983). The liquid magma viscosity was calculated by using the model of Shaw (1972), and the effect of crystals was estimated from the Einstein–Roscoe equation. The density of magma was modeled by an equation for silicate liquids of Lange and Carmichael (1987) which was corrected for the crystal content based on the crystal volumetric fraction ϕ_c.

The input data for magma ascent modeling consist of magma chamber pressure P_0 and temperature T, magma composition and crystal content, particle or pyroclast size d_p above the magma fragmentation level, conduit length L, and conduit diameter D. These conditions for Palizzi and 1888–1890 eruptions of Vulcano are shown in Tables 1 and 2, and were determined based on the volcanological and petrological data pertaining to the eruption of Palizzi, geothermal drill wells and seismic data, and were extrapolated to the Modern cycle by changing only the crystal content of magma to zero, reflecting the aphyric nature of the ejecta.

Crystal content

The crystal content of the wet-surge deposits of the eruptive cycles varies from 5 to 15 vol.% (Dellino et al., 1990), with the wet-surge samples being taken from the near-vent deposits. The characteristic features of these surges are their small mobility and their highly plastic behavior ("quaquaversal" structures and absence of settling in deposits). This implies that such a range of crystal content may represent an effective magmatic value which, together with the maximum crystal content of lava flows at Vulcano of about 20 vol.% (Castellet y Ballarà et al., 1982), suggests an appropriate crystal content during the magmatic eruption of Palizzi of about 10 vol.%. The main crystal phases are clinopyroxene and alkali feldspar (including sanidine). Extrapolation of data from Keller (1980), Castellet y Ballarà et al. (1982) and Frazzetta et al. (1983) suggests that clinopyroxene comprises about 60 vol.% of the total crystal content.

Magma chamber depth

Magma chamber depths during the Palizzi and last eruptions of Vulcano may be estimated from geothermal and seismic data. The Isola di Vulcano 1 (IV1) geothermal well near Grotta dei Palizzi reached a depth of 2050 m and encountered a monzogabbroic intrusion (dated at about 30,000 years ago) at 1360 m (Faraone et al., 1986), implying that no magma chamber has been stationed above the intrusion and that at present a magma chamber should lie below about 2000 m. However, the smoothing of the seismic waves between 3 and 4 km below La Fossa crater suggests the presence of a magma body of a small spatial extent underlaying the intrusion (Ferrucci et al., 1991). Accordingly, the magma chamber depth may be parametrized between 3 and 4 km (Table 2).

Magma chamber pressure

Magma chamber pressure P_0 was determined from the magma chamber depth and stratigraphy from the IV1 geothermal well, i.e.

$$P_0 = \int_0^L \rho_{cr} g \, dz + P_{atm}$$

where ρ_{cr} is the country rock density estimated from the drill (Fig. 3) (Faraone et al., 1986) to a depth of 2050 m. Beyond this depth, the density was assumed to correspond to the monzogabbroic intrusion density of 2750 kg/m^3 up to 4 km depth. Magma chamber pressures computed in this manner and corresponding to different conduit lengths are indicated in Table 2.

Table 2
Input parameters for magma ascent modeling for the Palizzi (P) pumice phase and 1888–1890 (1890) bread-crust bombs phase. These parameters consist of magma composition, crystal volumetric fraction ϕ_c, conduit length L, magma chamber pressure P_0, magma temperature T, pyroclast or particle diameter d_p, conduit diameter D, and dissolved water content in magma Y_0

	I	II	III	IV	V	VI
Eruption:	P/1890	P/1890	P/1890	P/1890	P/1890	P/1890
ϕ_c (vol.%)	10/0	10/0	10/0	10/0	10/0	10/0
L (km)	3	3.5	4	3	3.5	4
P_0 (MPa)	79.48	92.95	106.43	79.48	92.95	106.43
T (K)	1173, 1273	1173, 1273	1173, 1273	1173, 1273	1173, 1273	1173, 1273
d_p (μm)	200	200	200	200	200	200
D (m)	60	60	60	25	25	25
Y_0 (wt.%)	1	1	1	2	2	2

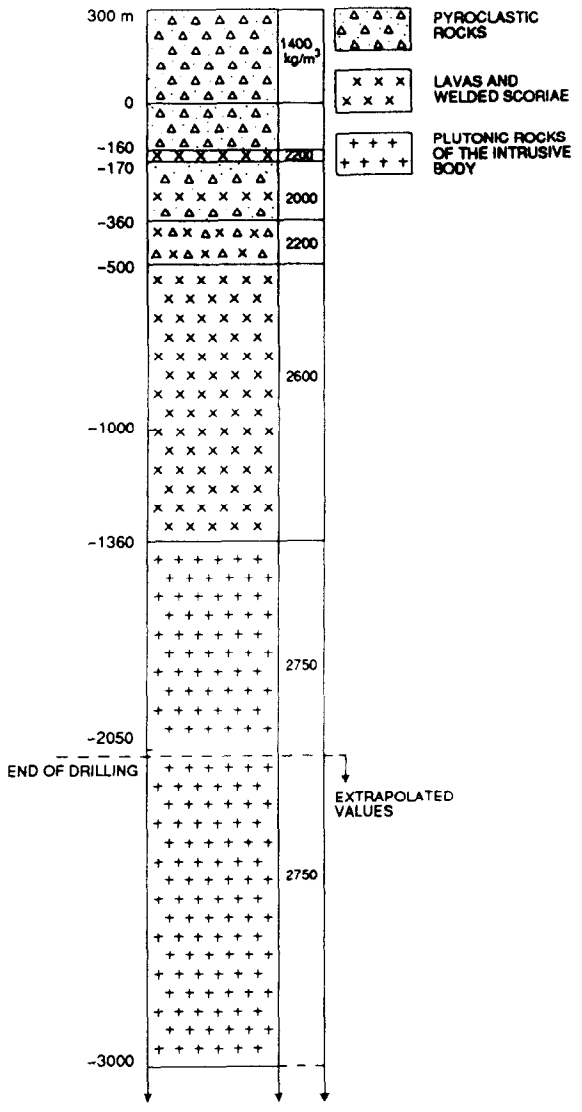

Fig. 3. Stratigraphy of Isola di Vulcano 1 geothermal well (modified after Faraone et al., 1986).

Magma temperature

Typical eruption temperatures for trachytes and rhyolites lie in the ranges 1173–1273 K and 1073–1173 K, respectively (McBirney, 1979; Cas and Wright, 1987). However, recent estimates for Vulcano's magmas suggest average temperatures of 1353 for trachytes and 1223–1273 K for rhyolites (Gioncada and Sbrana, 1993). Given this wide variation of temperatures, we parametrized the temperatures of Palizzi and 1888–1890 magmas as 1173 and 1273 K.

Conduit diameter

It is reasonable to assume that the conduit diameter during the last eruption of Vulcano corresponded to the present day innermost vent diameter which is about 50 m (geological map, Keller, 1980). Based on the work of Frazzetta et al. (1983), the ancient Palizzi cycle crater had a diameter similar in shape and size to that of the modern cycle (about 500 m) which includes the last eruption. Therefore, it is also reasonable to assume a conduit diameter for the Palizzi cycle of about 50 m. The conduit diameters of 60 and 25 m selected for magma ascent modeling in Table 2 embrace the 50-m value and reflect the constraints on the dissolved water content of the magma as discussed below.

Water content

The dissolved water contents of erupted magmas at La Fossa can be parametrized from examples of experimental petrology. The first example consists of an andesite suite of Paricutin volcano (Eggler, 1972), whereas the second example comes from the analysis of erupted basic products of Vesuvius in 1944 (Dolfi and Trigila, 1978). The former experimental studies established the dissolved water content of 2.2 wt.% at $T = 1373$ K and pressures up to 1,000 MPa (Eggler, 1972), whereas the latter experiments established a water content of 1.1 wt.% at $T = 1378$ K and $P = 50$ MPa (Dolfi and Trigila, 1978). Moreover, recent fluid inclusion studies suggest that the dissolved water contents of La Fossa magmas range from 1 to 1.5 wt.% (Clocchiatti et al., 1993). Based on the above information the dissolved water contents for Palizzi and Modern cycles of Vulcano can be constrained within 1–2 wt%.

Particle diameter

A particle size of $d_p = 200$ μm after magma fragmentation was used in the magma ascent and pyroclastic dispersion modeling, as suggested by the granulometric studies of pyroclastic flow and ash cloud deposits of Mt. St. Helens eruption in 1980 which give a median size between 300 and 600 μm for the former and between 39 and 68 μm for the latter (Kuntz et al., 1981). The above value of particle size was also found to be adequate in magma ascent modeling at Vesuvius and Mt. St. Helens (Papale and Dobran, 1993, 1994). The plinian eruption columns exhibit, however, particle sizes from few microns to several centimeters, with

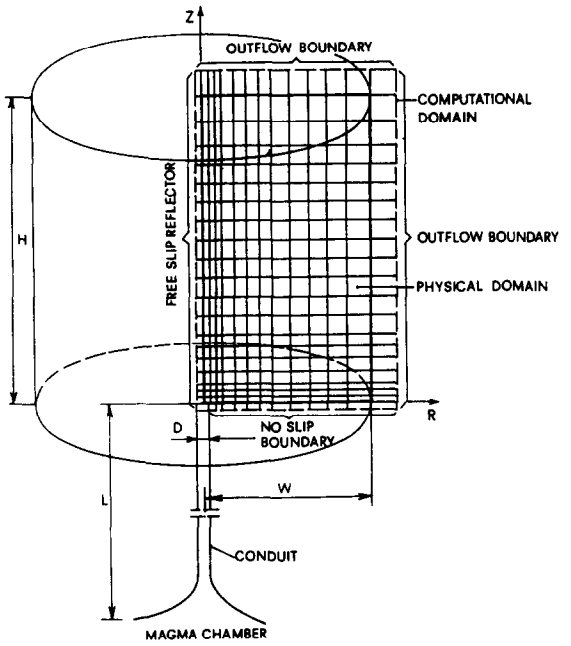

Fig. 4. Illustration of the physical and computational domains in an axisymmetric flow configuration above a volcanic vent. A two phase flow mixture of water vapor and pyroclasts (solid particles) exits from a vent of diameter D and mixes with the pressure- and temperature-stratified atmosphere above the vent. The physical domain has a radial extent W and a vertical extent H. The computational domain is two cells wider than the physical domain in the radial and vertical extents. The description of different types of boundary conditions shown in the figure is discussed in the text (after Dobran et al., 1993).

about 90 wt.% of solids exhibiting a particle size less than 5 cm and 40 wt.% less than 600 μm (Sparks and Wilson, 1976). The mean particle size of 200 μm appears, therefore, reasonable for modeling eruptions which produce collapsing columns and pyroclastic flows and underestimates the mean particle size of plinian-type columns.

3.2. Pyroclastic dispersion modeling and input data for simulations

The physical model of volcanic columns of Dobran et al. (1993) involves the conservation of mass, and balance of momentum and energy equations for the gas and pyroclasts phases. The gas phase consists of air and water vapor which allows for the mixing of water vapor exiting from a vent with a pressure- and temperature-stratified atmosphere. The pyroclasts are modeled as solid particles of a single granulometric size class as used in the magma ascent model above the magma fragmentation level in the conduit. The use of momentum and energy equations for each phase separately allows for the mechanical and thermal nonequilibrium between the phases. The gas turbulence is modeled by a turbulent subgrid scale model, whereas the effect of particle interaction in the flow is modeled by a granular flow model based on kinetic theory. The granular flow model accounts for the pyroclasts pressure and viscosity due to particle collisions and is useful for modeling the jet thrust region of the column and pyroclastic flows produced from partial or total column collapses.

The physical modeling equations used in the present work involve an ideal gas equation of state for the gas phase, constant molecular viscosity and thermal conductivities of gas and pyroclasts, and temperature-dependent specific heats of air and water vapor. The solution of the mass, momentum and energy balance equations of each phase was performed in a two-dimensional axisymmetric flow configuration above the volcanic vent as shown in Fig. 4, with an average topography representing La Fossa Cone. The physical domain in numerical computations involved a radial extent $W=1$ km and vertical extent $H=3$ km above sea level. The computational grid size ranged from 10 to 20 m which was previously found to be adequate to resolve the important characteristics of many simulated volcanic columns (Dobran et al., 1993). The volcanic vents in the simulations were located at 300 m altitude

Table 3
Vent parameters for volcanic column modeling of the Palizzi pumice fall phase determined from the magma ascent modeling in volcanic conduits of Vulcano. These parameters consist of gas and pyroclast temperature T, pressure P_v, gas velocity v_{gv}, pyroclast velocity v_{pv}, pyroclast size d_p, pyroclast density ρ_p, and pyroclast volumetric fraction ϵ_{pv} which for 60- and 40-m diameter conduits correspond to 1 and 2 wt.%, respectively, for the dissolved water content in the magma. The mass eruption rate was determined from modeling

Conduit diameter D (m)	60	40
Temperature T (K)	1173	1173, 1273
Pressure P_v (MPa)	0.32	0.92
Gas velocity v_{gv} (m/s)	125	155
Pyroclast velocity v_{pv} (m/s)	95	130
Pyroclast size d_p (μm)	200	200
Pyroclast density ρ_p (kg/m^3)	2530	2530
Pyroclast volumetric fraction ϵ_{pv}	0.034	0.043
Mass eruption rate M (kg/s)	2.32×10^7	1.82×10^7

and no allowance was made for the presence of craters above the vents. The effect of a crater above the conduit exit is to reduce the pressure of the gas-pyroclast mixture exiting from the vent and thus affect the thrusting of the volcanic jet into the atmosphere (Kieffer and Sturtevant, 1984). However, because of the conversion of gas pressure at the exit of a vent into the kinetic energy of gas and pyroclasts at the exit of a crater, the net result on the column dynamics should not be very significant. The boundary conditions corresponded to no mass, momentum, and energy fluxes across the axis of symmetry, and a no slip condition along and heat transfer perpendicular to the slopes of the volcano. At the free-flow boundaries (see Fig. 4), the boundary conditions corresponded to the free outflow and inflow of the gas and pyroclasts, whereas at the volcanic vent the pyroclast volumetric fraction, pressure, and gas and pyroclasts velocities and temperatures as determined from magma ascent modeling were assumed constant during each simulation, from the time of initial thrusting of gas and pyroclasts into the atmosphere to the time when the volcanic column and ground flow covered the entire physical domain. The input data at the vent for volcanic column modeling are summarized in Table 3.

4. Results

Figures 5–8 illustrate the magma ascent results for the Palizzi pumice fall. Figure 5 shows the gas volumetric fraction and pressure variations along the conduit for a conduit diameter of 60 m, magma temperature of 1173 K, 1 wt.% of dissolved water, and conduit lengths of 3, 3.5 and 4 km (cases I, II, and III in Table 2). The pressure distribution shown in the figure is nondimensionalized with respect to the lithostatic pressure P_0 corresponding to the conduit length L, whereas the dashed line corresponds to the lithostatic pressure. The fluid pressure in the conduit remains below the lithostatic pressure for all conduit lengths considered. The maximum difference between the lithostatic and fluid pressures is about 14 MPa for all conduit lengths and occurs at the magma fragmentation level which corresponds to the gas volumetric fraction $\alpha = 0.75$. The results in Fig. 5 also show that increasing the conduit length from 3 to 4 km produces a decrease in the magma fragmentation depth from 630 to 600 m and an

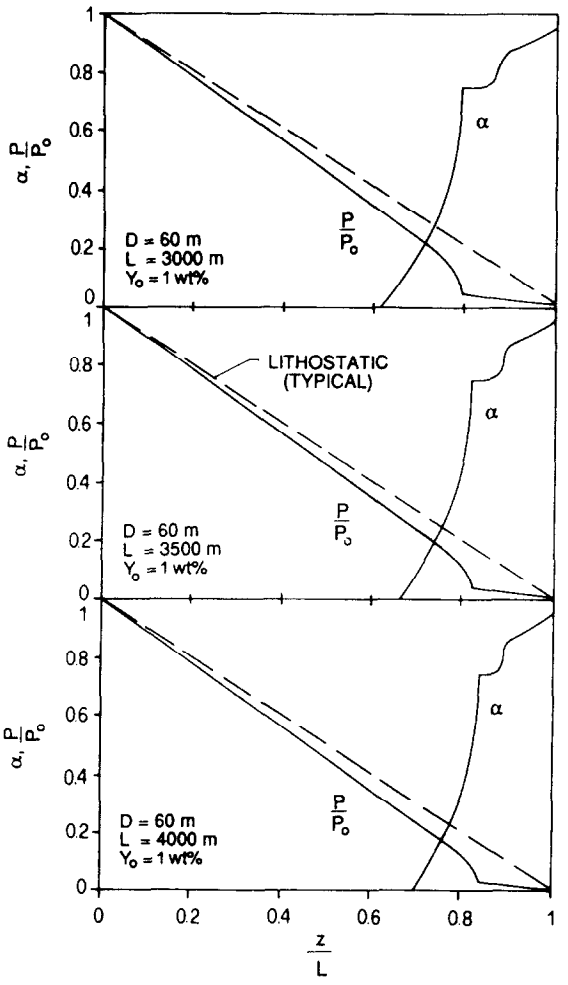

Fig. 5. Pressure and gas volumetric fraction variations along conduits of 3, 3.5 and 4 km lengths, with 60 m diameter, erupting magma at a temperature of 1173 K, and with 1 wt.% of dissolved water in the magma (cases I, II, and III for Palizzi in Table 2).

increase of the gas exsolution depth from 1140 to 1160 m. The results for the 25-m conduit diameter, magma temperature of 1173 K, 2 wt.% dissolved water, and conduit lengths of 3, 3.5 and 4 km are shown in Fig. 6 (cases IV, V, and VI in Table 2). In this case, the maximum difference between the lithostatic and magmatic pressures at the magma fragmentation level is about 28 MPa for all conduit lengths, and the magma fragmentation and exsolution depths increase from 1260 to 1360 m and from 1800 to 1880 m, respectively.

Figure 7 shows a more detailed comparison between the results in Figs. 5 and 6. Also shown are the pressure distributions close to the conduit exits and the effect of

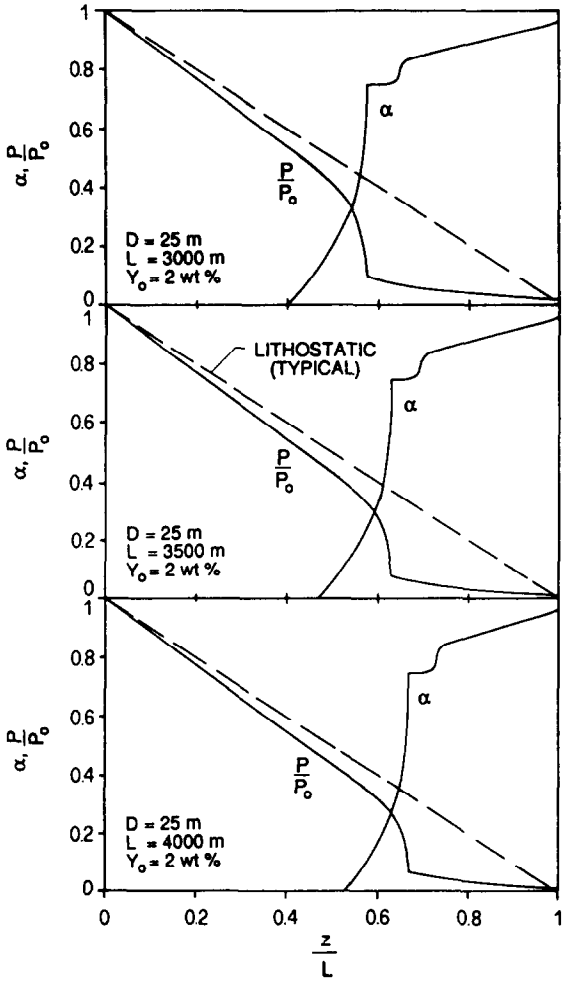

Fig. 6. Pressure and gas volumetric fraction variations along conduits of 3, 3.5 and 4 km lengths, with 25-m diameter, erupting magma at a temperature of 1173 K, and, with 2 wt.% of dissolved water in the magma (cases IV, V and VI for Palizzi in Table 2).

conduit lengths on these distributions. A 25-m conduit diameter and 2 wt.% dissolved water produces larger exit pressures, and larger magma fragmentation and exsolution depths for all conduit lengths than a 60-m conduit diameter and 1 wt.% of dissolved water in the magma. The smaller conduit diameter also produces larger vent exit velocities and gas volumetric fractions which favor the formation of a buoyant column (Neri and Dobran, 1994). The magma ascent model failed, however, to produce physical results of choked and nonchoked flow (with exit pressure equal to or greater than the atmospheric pressure) of fragmented magma through the conduit pertaining to a diameter of less than 60 m and 1 wt.% of dissolved water. For 2 wt.% of dissolved water in the magma, the model also failed to produce solutions for conduit diameters of less than 25 m. The results thus show that a 60-m conduit diameter is the minimum diameter which is compatible with 1 wt.% of dissolved water in the magma, whereas a 25-m conduit diameter requires a minimum dissolved water in the magma of 2 wt.% to sustain a magmatic eruption with magma fragmentation within the conduit. The mass eruption rates for the 60- and 25-m conduit diameters are: 2.4×10^7 kg/s (case I), 2.3×10^7 kg/s (case II), 2.2×10^7 kg/s (case III), 4.6×10^6 kg/s (case IV), 4.4×10^6 kg/s (case V), and 4.3×10^6 kg/s (case VI).

The effect of increasing the magma temperature to 1273 K on the pressure and gas volumetric fraction distributions along the conduit is illustrated in Fig. 8. This magma temperature produces pressures larger than lithostatic in almost all regions of the conduit, except near the magma fragmentation level where the magma pressure falls below the lithostatic pressure by about 1 MPa for the 60-m conduit diameter and 1 wt.% of dissolved water, and about 8 MPa for the 25-m conduit diameter and 2 wt.% dissolved water. The corresponding magma fragmentation depths are about 100 and 450 m.

The pressure and gas volumetric fraction variations along the conduits of 3 km length, 25-m and 60-m conduit diameters, magma temperature of 1173 K, and 1 and 2 wt.% of dissolved water conditions during the bread-crust bombs phase of the last eruption of Vulcano are illustrated in Fig. 9. As seen from this figure, these conditions produce large pressures and low gas volumetric fractions at the exits of conduits. For the 60-m conduit diameter and 1 wt.% dissolved water, the vent pressure is about 14 MPa, the gas volumetric fraction about 0.3, and the mass discharge rate about 70 kg/s, whereas for the 25-m conduit diameter and 2 wt.% dissolved water the values are about 20 MPa, 0.5 and 20 kg/s. These values imply that, in both cases, the exiting magma remains unfragmented and discharging at rates comparable to very low rates of lava extrusion. For the 25-m conduit diameter and 1 wt.% dissolved water, the magma ascent results (not illustrated) show that the vent exit pressure and gas volumetric fraction are about 16 MPa and 0.4, respectively. By changing the magma temperature to 1273 K, the modeling results for the 60-m conduit diameter and 1 wt.% of dissolved

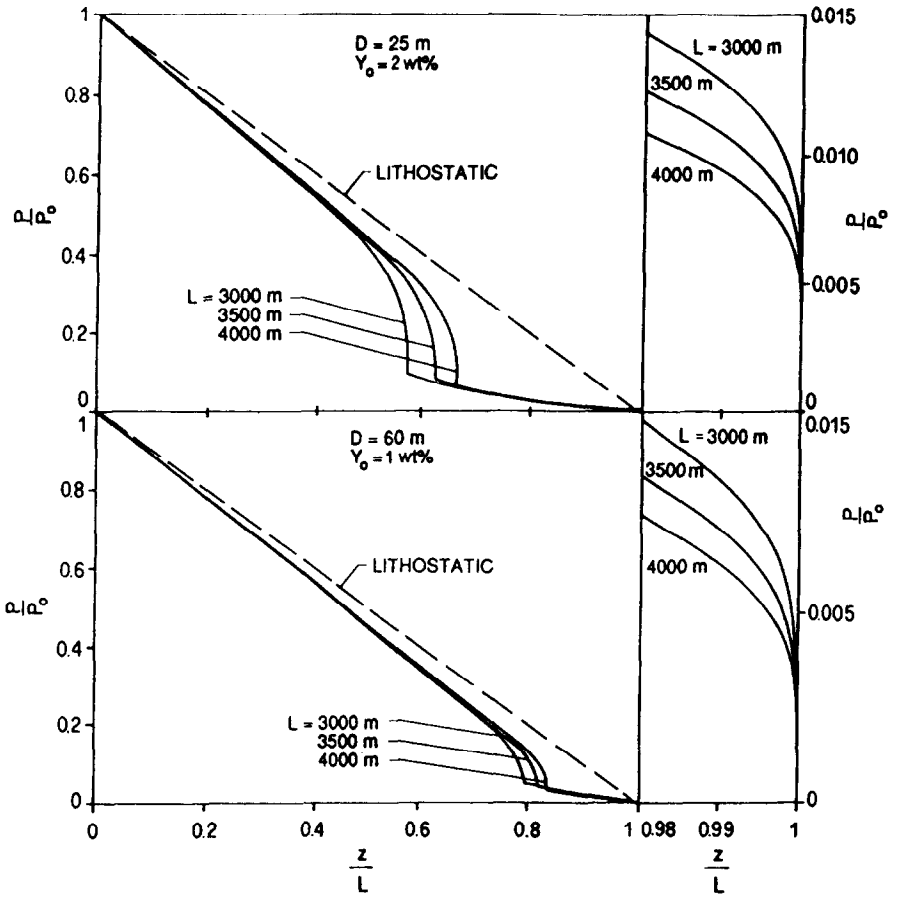

Fig. 7. Comparison between pressure variations along conduits of 3, 3.5 and 4 km lengths, with 25- and 60-m diameters, erupting magma at a temperature of 1173 K, 1 and with 2 wt.% of dissolved water in the magma for the Palizzi pumice fall eruption phase.

water produce conduit exit pressure of 14 MPa, a gas volumetric fraction of 0.1, and very low velocities. A temperature of 1273 K, 25-m conduit diameter, and 1 and 2 wt.% dissolved water produce, however, magma fragmentation very near the conduit exit, exit pressures of about 7 and 0.3 MPa, and exit velocities of about 0.4 and 1 m/s, respectively. As discussed below, high exit pressures and low gas volumetric fractions favor the production of bread-crust bombs which occurred after dry-surges and flows during the last eruption of Vulcano.

The results for the Palizzi pumice fall phase and an erupting magma temperature of 1173 K illustrated in Figs. 10–14 show the time-wise distributions of pyroclast volumetric fractions and velocities, and of gas temperatures, of two different volcanic columns corresponding to the vent parameters in Table 3. The volcanic column in Figs. 10–12 corresponds to the 60-m conduit diameter and 1 wt.% dissolved water. At about 20 s after the gas-pyroclast mixture exits from the vent, the two-phase flow jet loses its vertical thrust at about 700 m above the vent by forming a fountain and begins collapsing. At 30 s after the eruption, the collapsing part of the column becomes evident as shown by the particle velocity vector plot in Fig. 11a, whereas at 40 s the collapsed portion of the column begins spreading along the slopes of the volcano by forming a ground flow which is very dilute and thick (Fig. 10). Above the fountain the rising water vapor cloud entrains some particles and continues to rise as a dilute buoyant plume (Figs. 10, 11b) which after 90 s reaches a height of about 2 km above sea level with a very strong upward flow (Fig. 11c). By this time a co-ignimbrite or phoenix cloud (Dobran et al., 1993), formed at the break-

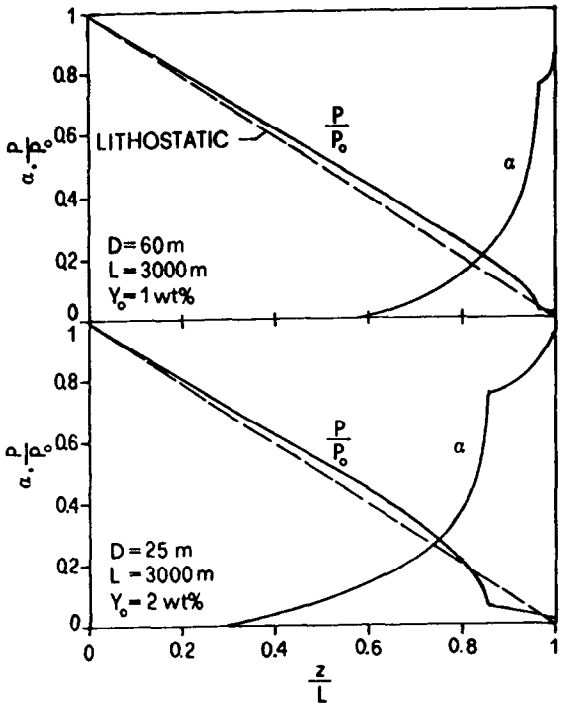

Fig. 8. Comparison between pressure and gas volumetric fraction variations along a conduit 3 km long, with 25- and 60-m diameters, erupting magma at a temperature of 1273 K, and with 1 and 2 wt.% of dissolved water in the magma for the Palizzi pumice fall eruption phase (cases I and IV in Table 2).

in-slope of the volcano at about 60 s, is seen merging with the collapsing portion of the column and forming a large volcanic plume above the island. After the column collapses at about 40 s, the fountain assumes a narrow shape and builds a ground flow traveling at about 60 m/s along the upper slopes of the volcano (Figs. 11b,c). The temperature distribution of this volcanic column (Fig. 12) shows that the ground flow causes very high temperatures along the slopes of the volcano.

The evolution of the volcanic column corresponding to the 40-m conduit diameter, a magma temperature of 1173 K, and 2 wt.% dissolved water is shown in Figs. 13 and 14. This volcanic column has a different behavior from that of the preceding column, since the jet portion of the column manages to entrain and heat a sufficient quantity of air to make the column buoyant and thus prevent its total collapse. The part of the column shown collapsing at 55 s at about 600 m altitude is due to the high density of the central part of the column which loses its vertical momentum at about 1.5 km height. As this high-density mixture of gas and pyroclasts begins to descend it is pushed radially outward by the vertical thrust of the volcanic jet. The lower collapsing part of the column is clearly shown at 70 s. At 90 s, the very-low-velocity (several m/s) ground flow produced from the collapsed portion of the column has merged with the noncollapsed portion of the column. Together these produce a large volcanic cloud with a radius of about 1 km. The upper part of the column continues to rise and after 90 s reaches a height of about 3 km above sea level (Fig. 13). By comparing the particle velocity vectors (Figs. 11 and 14) of the two volcanic columns it can be seen that the ground flow of the column corresponding to the 40-m conduit diameter has a much smaller momentum than that of the flow of the column corresponding to the 60-m conduit diameter, and that the former column is much more buoyant. A 40-m conduit diameter, 2 wt.% dissolved water, and an erupting magma temperature of 1273 K produce similar column characteristics but the column

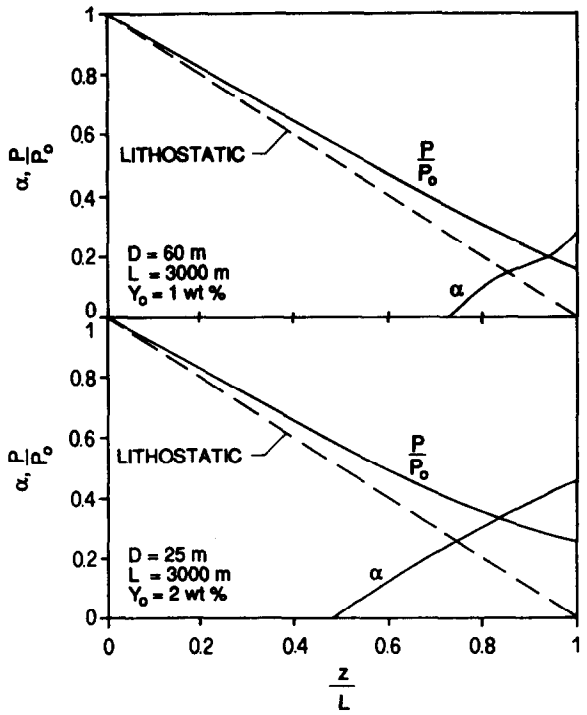

Fig. 9. Pressure and gas volumetric fraction variations along conduits of 3 km length, with 60- and 25-m diameters, erupting magma at a temperature of 1173 K, and with 1 and 2 wt.% of dissolved water in the magma (cases I and IV for the 1890 eruption in Table 2).

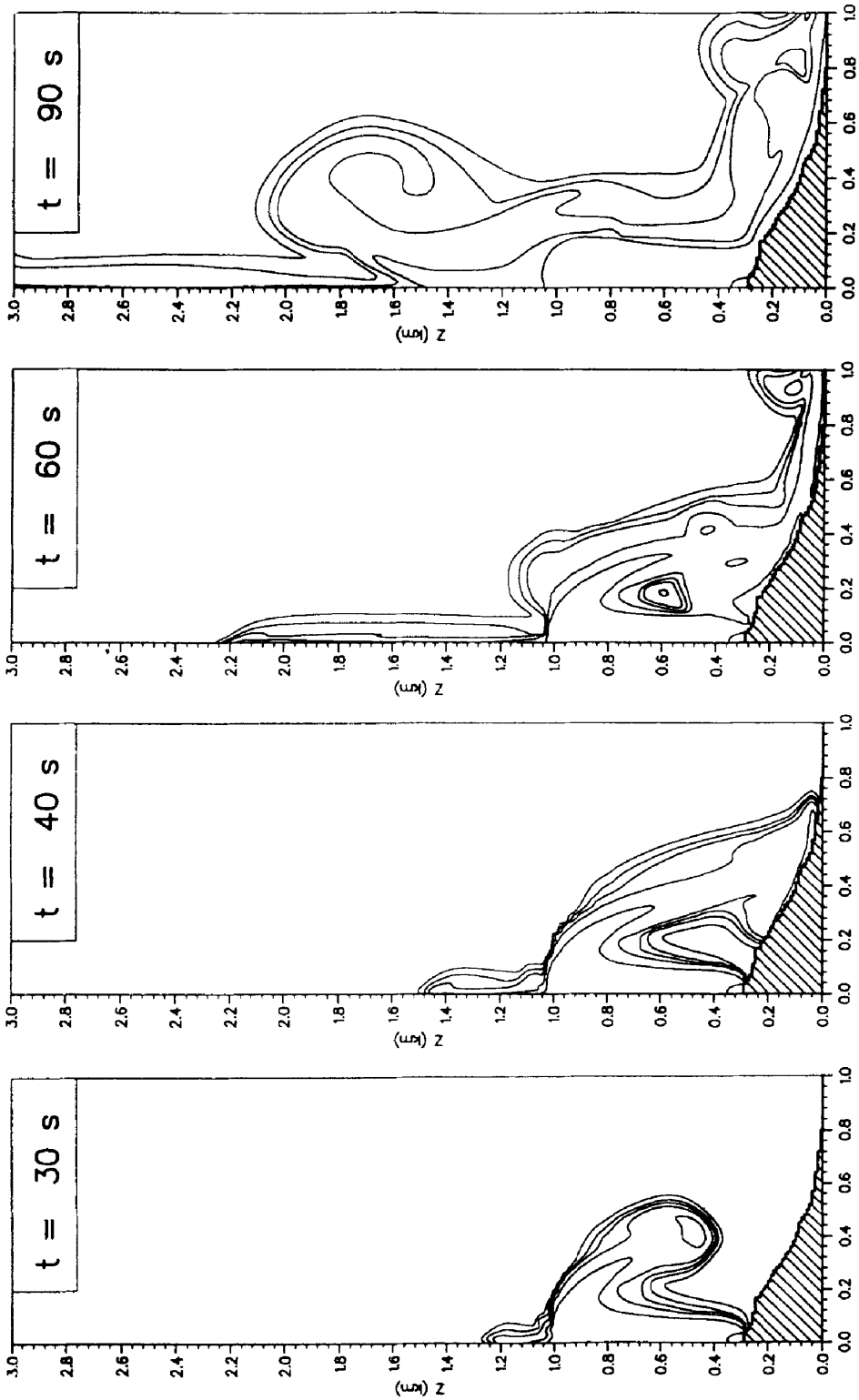

Fig. 10. Distribution of particle volumetric fraction in the atmosphere at 30, 40, 60 and 90 s after the gas-pyroclast mixture exits from a 60-m diameter conduit. The contour levels shown are the exponents to the base 10 and, beginning from the outer or more distant from the vent region, correspond to -8, -6, -5, -4, -3, -2 and -1. The vent conditions in this and subsequent figures are summarized in Table 3.

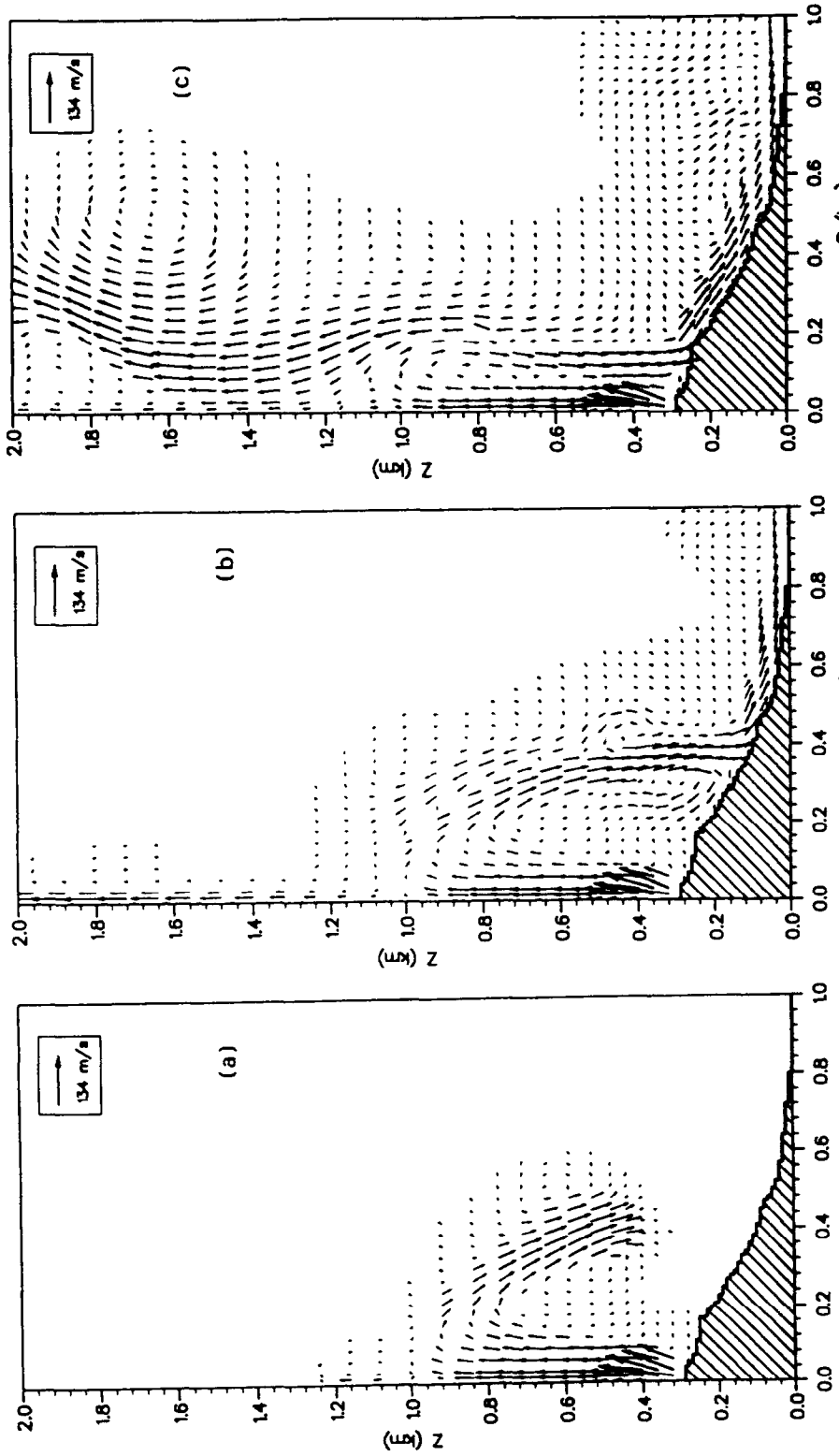

Fig. 11. Particle velocity vector plots of the volcanic column corresponding to a 60-m diameter conduit. The plots correspond to: (a) 30 s, (b) 60 s and (c) 90 s time frames. The velocities which are 100 times less than the one reported in the box inserted in the figure are not shown.

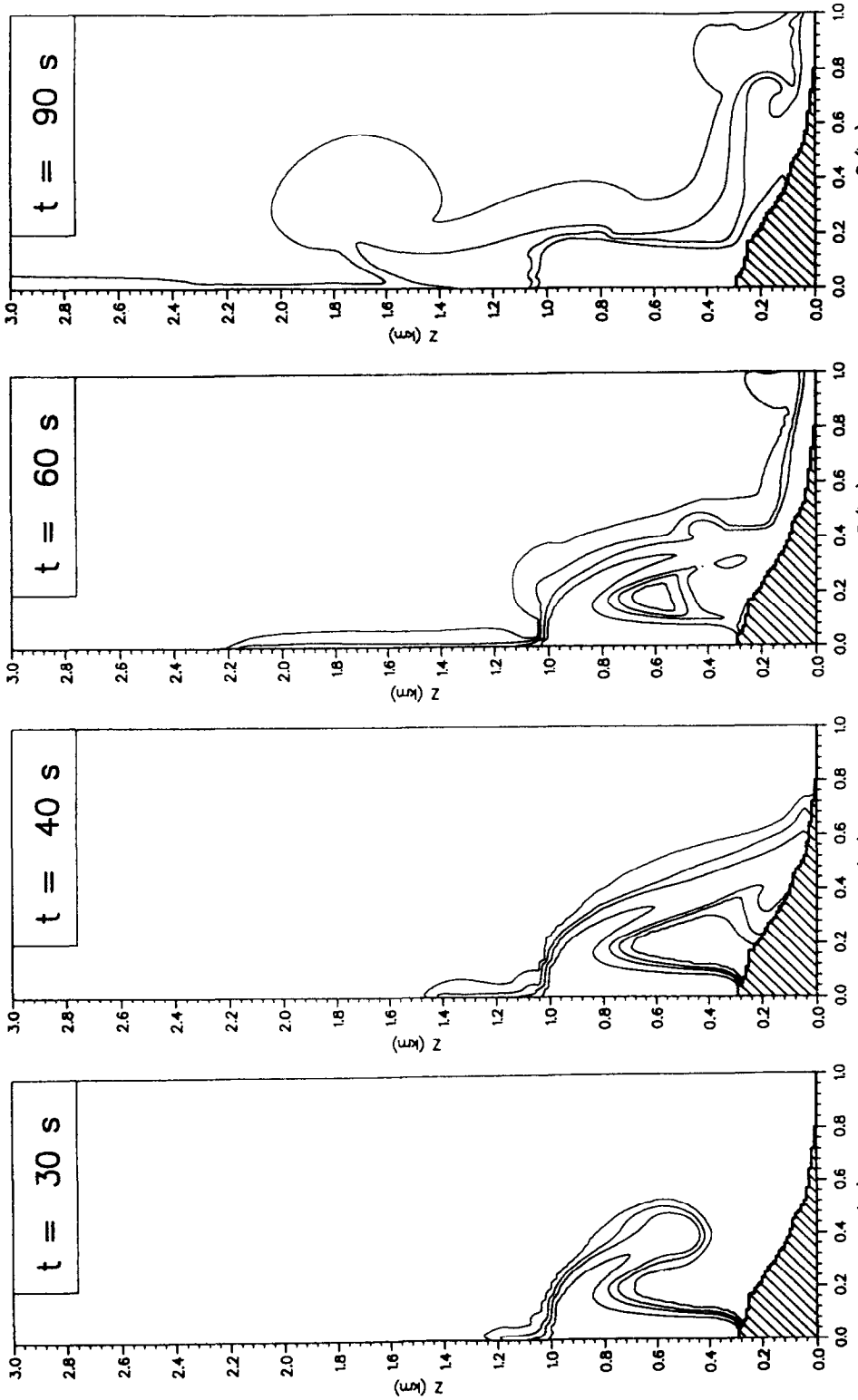

Fig. 12. Distribution of gas temperature at 30, 40, 60 and 90 s after the gas-pyroclast mixture exits from a 60 m diameter conduit. A contour level in the figure represents the difference between the local gas temperature and the undisturbed atmospheric air temperature at $Z = 0$. The temperature contours, beginning from the outer or more distant from the vent region, correspond to 0, 200, 500 and 800 K.

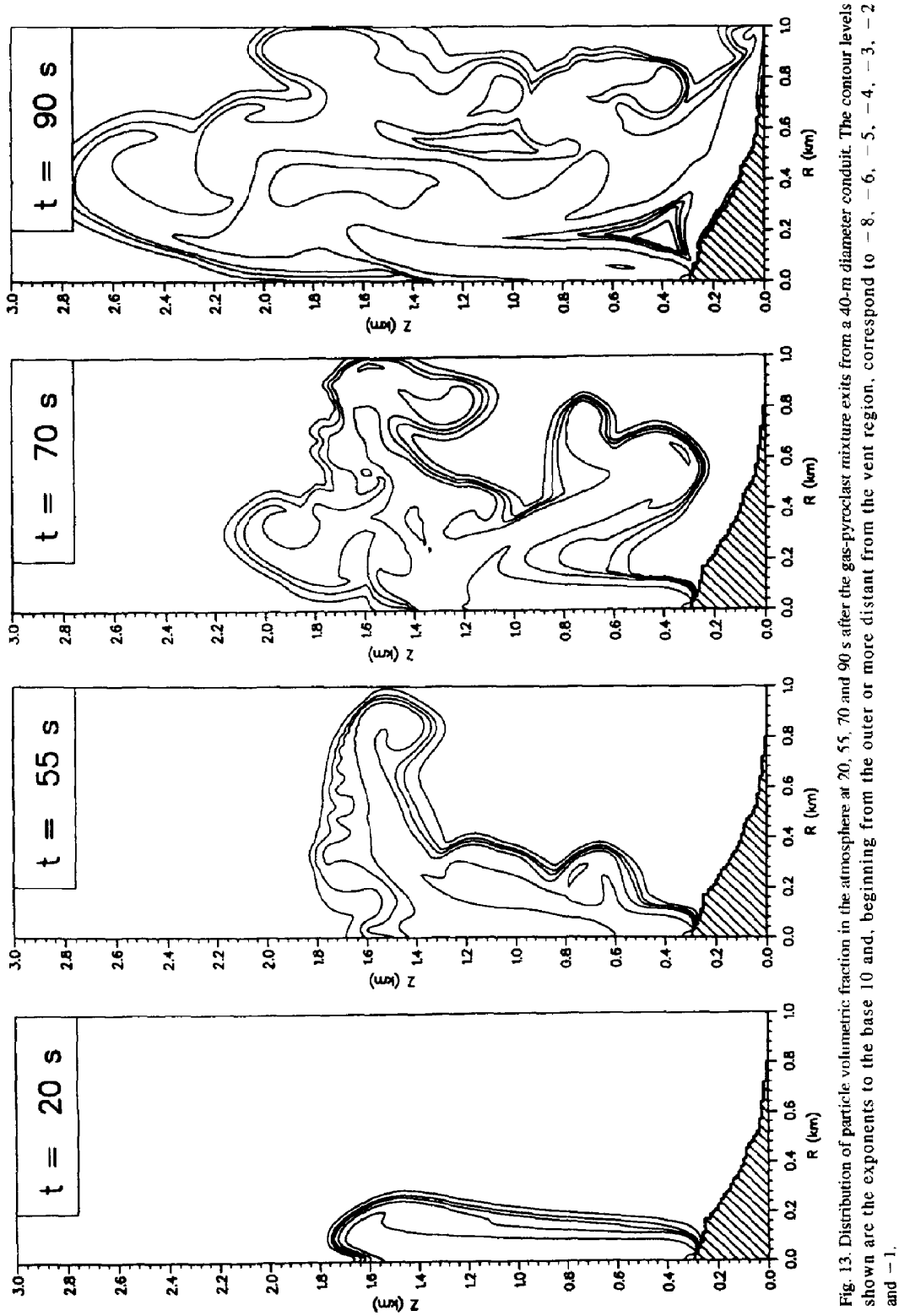

Fig. 13. Distribution of particle volumetric fraction in the atmosphere at 20, 55, 70 and 90 s after the gas-pyroclast mixture exits from a 40-m diameter conduit. The contour levels shown are the exponents to the base 10 and, beginning from the outer or more distant from the vent region, correspond to -8, -6, -5, -4, -3, -2 and -1.

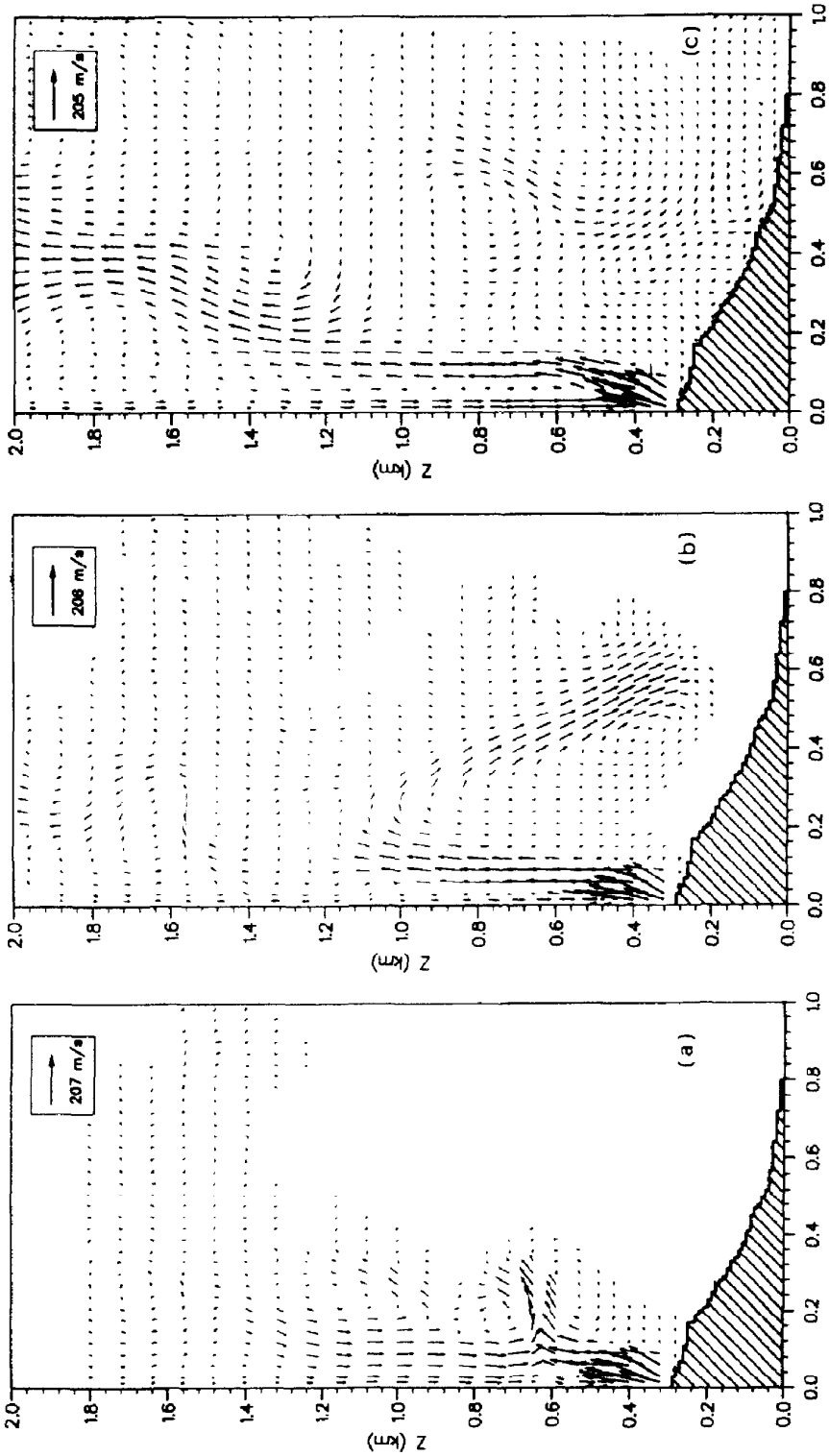

Fig. 14. Particle velocity vector plots of the volcanic column corresponding to a 40-m diameter conduit. The plots correspond to: (a) 55 s, (b) 70 s and (c) 90 s time frames. The velocities which are 100 times less than the one reported in the box inserted in the figure are not shown.

is more buoyant than that corresponding to the magma temperature of 1173 K.

From the volcanic column simulations it is evident that different conduit and magma characteristics can produce different behaviors of volcanic columns; in one case producing a collapsing column which builds a ground flow whereas in the other case producing a more sustained column which tends to rise as a plinian column. As further discussed below, the deposits associated with the Palizzi pumice fall and the results from volcanic column simulations may be employed as constraining parameters for establishing possible magmatic conditions during this eruption phase.

5. Discussion

The magma ascent and pyroclast distribution modeling results suggest that the phreatic, phreatomagmatic, magmatic and lava flow activities during each eruptive cycle of Vulcano are a consequence of different magma compositions within the volcanic system and the existence of aquifers within the changing structural characteristics of magma ascent pathways.

The petrological, volcanological and magma ascent modeling constraints indicate that the Palizzi magmatic eruption is more consistent with cases IV, V and VI than with cases I, II and III in Table 2 for both temperatures. The wet- and dry-surges preceding the Palizzi pumice fall are associated with phreatomagmatic events (Frazzetta et al., 1983), implying the presence and opening of aquifers prior to the Palizzi magmatic eruption. Moreover, the stratigraphic analyses of Volcano Porto 1 and Isola di Vulcano 1 geothermal wells established the presence of altered lavas at a depth of about 1300 m (Gioncada and Sbrana, 1991) and breccias from 1060–1073 m (Faraone et al., 1986) below the present crater location, indicating that these lavas and breccias were alterated by circulating acidic fluids. The mineralogical data on wet surges of La Fossa Cone also indicate that a mixing between deep acidic gases t and water is capable of producing rapid alterations of volcanic rocks (Capaccioni et al., 1991). Moreover, geochemical analyses of fumaroles and waters from shallow wells and studies of the altered rocks from geothermal wells suggest the presence of permeable rocks which contain rain water at shallow depths and salty waters or brines at greater depths (Mazor et al., 1988; Chiodini et al., 1991; Gioncada and Sbrana, 1993). Combining these data it is likely that the aquifers on the island of Vulcano exist up to at least 1300 m depth which is consistent with the locations of magma fragmentation levels predicted by the magma ascent modeling. For an erupting magma temperature of 1173 K, a 25-m conduit diameter and 2 wt.% of dissolved water in the magma, the predicted magma fragmentation level is at about 1300 m, whereas for the same erupting magma temperature, 60-m conduit diameter and 1 wt.% of dissolved water in the magma this level is at about 600 m below the crater rim. The erupting magma temperature of 1273 K and conduit diameters of 60 and 25 m decrease the magma fragmentation depths to 450 and 100 m, respectively. With a low-temperature magma, there may thus be a considerable decrease of magmatic pressure below the lithostatic pressure at the magma fragmentation level which can precipitate inward wall collapses and efficient water pouring into conduits causing magma–water interaction (Dobran, 1992; Dobran and Papale, 1993). With a high-temperature magma, however, the magma pressure exceeds the lithostatic pressure in almost all regions of the conduit (Fig. 8), and there should be a lower probability of magma interacting efficiently with underground aquifers due to the difficulty of producing outward wall collapses and opening of these aquifers. The difference between the lithostatic and magmatic pressures at the magma fragmentation levels varies from 14 to 28 MPa for a magma temperature of 1173 K and 1 to 8 MPa for a magma temperature of 1273 K. The presence of amphibole and mica crystals in the mineral phases of the Palizzi pumice fall (Frazzetta et al., 1983) under the conditions of pressure and temperature discussed in section 3.1 and the very small predicted difference between the lithostatic and magma pressures for conduit diameter of 60 m, erupting magma temperature of 1273 K, and dissolved water content of 1 wt.%, implies that the magma erupting during this phase had a dissolved water content which is closer to the upper limit of the selected range. These results, together with the volcanic column results discussed below, suggest that the magmatic eruption of Palizzi causing the pumice fall occurred from a conduit of diameter about 30 m and involved 2 wt.% of dissolved water in the magma rather than a larger conduit diameter and smaller dissolved water content.

As indicated in section 2.1, the Palizzi and underlying phreatomagmatic deposits are undisturbed and do not show evidence of erosion at their top surfaces. This suggests that the volcanic column of Palizzi did not produce ground flows which can cause erosional features because of the large velocities along the slopes of the volcano and that the deposit was primarily produced by fall of pyroclasts from the volcanic column. The modeling results related to the volcanic columns with 40-m conduit diameter, 2 wt.% dissolved water, and erupting magma temperatures of 1173 and 1273 K are in accord with the volcanological data, whereas the results pertaining to the volcanic column with a 60-m conduit diameter shown in Figs. 10–12 are not, since such a column produces: (1) ground flows with very low velocities which should not have been capable of eroding the phreatomagmatic deposits emplaced before the Palizzi pumice fall; and (2) a buoyant plume which has the tendency to produce primarily fall deposits. This consistency between the modeling predictions and field deposits further justifies the above conclusion that the magma which produced the Palizzi pumice fall eruption phase had a water content of about 2 wt.% and that the eruption occurred from a conduit with diameter 25–30 m.

The ejection of bread-crust bombs during the last eruption of Vulcano is consistent with the magma ascent modeling results of 60- and 25-m conduit diameters and 1 and 2 wt.% of dissolved water in the magma shown in Fig. 9 for an eruption temperature of 1173 K, and with the conduit diameter of 60 m and 1 wt.% of dissolved water in the magma for an erupting magma temperature of 1273 K, because of the ejection of magma at high pressure, low gas volumetric fraction, and at low velocities. For a magma temperature of 1273 K, a conduit diameter of 25 m, and 1 and 2 wt.% of dissolved water in magma, the magma ascent modeling results predicting magma fragmentation near the conduit exit do not, however, appear to be consistent with the presence of poorly vesiculated bread-crust bombs. This thus implies that the magma temperature of 1273 K used in modeling the bread-crust bombs phase during the last eruption of Vulcano is overestimated. With the magma temperature of 1173 K and using average values of gas-magma discharge rate of 50 kg/s and an exit gas volumetric fraction of 0.3 established from modeling, a magma density of 2500 kg/m^3, and a conduit diameter of 30 m, gives the magma velocity at the vent of about 0.01 mm/s. Such a low-velocity and high-pressure flow should produce an effective cooling of magma in the superficial regions of magma pathways and thus induce brittle failure of magma leading to the formation of large chunks of magma or bombs. The process should then repeat itself by the ascent of new magma into upper regions of magma pathways by cooling and brittle failure of this magma leading to the repetition of this cycle until the exhaustion of magma supply from depth. It should be noted that a trachytic magma may also produce chunks of magma in the manner indicated above if the conditions within the volcanic system (such as low ascent velocity and/or effective magma cooling by interaction with aquifers) favor brittle failure of magma. These conditions appear to have occurred during the Punte Nere cycle which produced trachytic block falls (Frazzetta et al., 1983).

The magma ascent and pyroclastic dispersion modeling results presented above, together with the volcanological and petrological data of La Fossa Cone eruptions, allow for better interpretation of these eruptions. On the basis of these results it is possible to argue that a *typical* eruption of Vulcano starts with a magma which channels its way toward the surface through one or more reservoirs which may or may not contain more viscous magma. The erupting magma ascends along the preceding and/or self generating fractures toward the surface and produces inward and/or outward conduit wall ruptures, depending on its physical properties such as viscosity and the mechanical conditions of the surrounding rocks, and it is able to promote an efficient magma–water interaction if water is available near the magma fragmentation level. The ascending trachytic magma at Vulcano appears at first to interact with aquifers until they are emptied (initial phreatic and phreatomagmatic phases of different cycles) (Barberi et al., 1988). If these aquifers are emptied before the supply of magma is exhausted, the eruption proceeds as a magmatic eruption, such as during the Palizzi and other cycles of Vulcano, until this magma is exhausted and more viscous rhyolitic magma from depth begins to rise along the conduit. The ascent of a more viscous magma appears to produce principally lava flows which usually terminate different cycles. The ejection of bread-crust bombs during the last eruption of Vulcano may be explained by the small availability of trachytic magma which was unable to produce sufficiently large pathways within the volcanic edifice for the subsequent

steady effusion of rhyolitic magma. The ascent of rhyolitic magma at low velocities and high pressures favors more rapid cooling and brittle failure of magma leading to the ejection of large chunks of magma. After the Palizzi cycle, the lavas at Vulcano consist of more evolved compositions than those producing wet- and dry-surges and flows, and their emplacement is consistent with the predictions of fluid-mechanics modeling of magma ascent. This appears to justify the hypothesis that each eruption cycle of Vulcano is initiated by a more basic magma which channels its way toward the surface through the more evolved and viscous magmas which remained from the preceding eruptive cycles and which erupt after the more basic magma has been exhausted. The ascent and quantity of basic magma entering from the feeding system of Vulcano, the differentiation processes of this magma at higher levels of the system controlled by the magma ascent pathways, and the surrounding aquifer conditions appear to be the main factors governing the eruptive phases during different eruptions of the volcano.

6. Summary and conclusions

The Palizzi and Modern cycles of Vulcano were studied by using two-phase flow models of magma ascent in volcanic conduits and pyroclast dispersion in the pressure- and temperature-stratified atmosphere. The input data for magma ascent modeling were constrained by petrological, volcanological and geophysical data, and the model was used to establish the locations of magma exsolution and fragmentation levels, and gas and pyroclasts velocities, pressures, and pyroclasts volumetric fractions at the exits of different diameter and length conduits. The vent exit conditions corresponding to the dispersed pyroclasts in the gas phase were employed in pyroclastic dispersion modeling to establish the distribution of gas and pyroclasts in the atmosphere and along the slopes of the volcano during the first few minutes after the eruptions.

The modeling results showed that the Palizzi pumice fall eruption phase is consistent with a magma containing about 2 wt.% of dissolved water and erupting from a conduit with a diameter of about 30 m. The predicted locations of magma fragmentation levels in conduits with lengths between 3 and 4 km established on the basis of geophysical data are in accord with the locations of altered lava layers and superficial aquifers obtained from the stratigraphical analysis of geothermal wells and geochemical data from fumaroles and shallow fresh water wells. The modeled volcanic column of this eruption is shown to produce a buoyant volcanic plume and a low velocity ground flow which is consistent with the Palizzi pumice fall data whereby the underlying phreatomagmatic flow deposits are undisturbed and do not show evidence of erosion at their top surfaces.

The magma ascent modeling of the bread-crust bombs phase of the last eruption of Vulcano predicted very low velocities of the ascending magma. Such flows, which are practically stationary, were shown to produce very high vent exit pressures (about 20 MPa) and low gas volumetric fractions (less than about 0.5), implying the difficulty of producing magma fragmentation during an open conduit condition and efficient magma–water interaction during this eruption. The flow of such a viscous magma through the upper pathways of the volcanic complex should favor an effective cooling and brittle failure of magma in the unconsolidated upper regions of the volcanic system. This brittle failure of magma may be responsible for the ejection of bread-crust bombs or chunks of magma.

The available volcanological, petrological and geophysical data, and the modeling results, permitted the establishment of an eruption scenario of each cycle of activity at Vulcano whereby the chemical and physical characteristics of new magma being supplied into the volcanic system and magma remaining in the system after previous eruptions, mechanical characteristics of the magma ascent pathways, and the conditions of aquifers surrounding these pathways determine the duration of phreatic, phreatomagmatic, magmatic and lava flow activities within each cycle. The reduction of trachytic products during the eruptive cycles of Vulcano and the dominance of rhyolitic products during the last eruption of the volcano imply a reduction of the basic magma supply into the volcanic system. Further understanding of various eruptive phases at Vulcano for the purpose of adequately assessing the volcanic hazard not only requires the development of magma–water interaction and hydrothermal circulation models, but also the collection of much more detailed modeling-oriented volcanological, petrological and geophysical data.

7. Nomenclature

d particle diameter
D conduit diameter
g gravitational acceleration
H vertical extent of physical domain (Fig. 4)
L conduit length (Fig. 1)
M mass eruption rate
P pressure
R radial coordinate
T temperature
v vertical component of velocity
Y dissolved water fraction in wt.%
z distance along the conduit
Z vertical coordinate above sea level
W radial extent of physical domain (Fig. 4)

Greek

α gas volumetric fraction
ϵ pyroclast volumetric fraction
ρ density
ϕ crystal volumetric fraction

Subscripts

atm atmospheric
c crystal
cr country rock
f fragmentation
g gas phase
o magma chamber location
p particles or pyroclasts phase
s exsolution
v vent

Acknowledgements

We wish to thank Paolo Papale for useful discussions regarding this work.

References

Barberi, F., Navarro, J.M., Rosi, M., Santacroce, R. and Sbrana, A., 1988. Explosive interaction of magma with ground water: insights from xenoliths and geothermal drillings. Rend. Soc. Ital. Miner. Petr., 43: 901–926.

Barberi, F., Neri, G., Valenza, M. and Villari, L., 1991. 1987–1991 unrest at Vulcano. Acta Volcanol., 1: 95–106.

Capaccioni, B., Coniglio, S. and Fratini, F., 1991. Clay minerals on recent products of hydromagmatic activity: considerations on their genesis. Acta Vulcanol., 1: 69–77.

Cas, R.A.F. and Wright, J.V., 1987. Volcanic Succession: Modern and Ancient. Allen & Unwin, UK, 528 pp.

Castellet y Ballarà, G., Crescenzi, R., Pompili, A. and Trigila, R., 1982. A petrological model on magma evolution of Vulcano eruptive complex (Aeolian Islands, Italy). A. Coradini and M. Fulchignoni (Editors), The Comparative Study of the Planets. D. Reidel Publ., Dordrecht, pp. 459–416.

Chiodini G., Cioni, R., Guidi, M. and Marini, L., 1991. Geochemical variations at Fossa Grande crater fumaroles (Vulcano Island, Italy) in summer 1988. Acta Vulcanol., 1: 179–192.

Clocchiatti, R., Gioncada, A., Mosbah, M. and Sbrana, A., 1993. Studio delle inclusioni vetrose nei prodotti di Vulcano (Eolie): primi dati sul contenuto pre-eruttivo in elementi volatili (H_2O, S, Cl, F) dei magmi di Vulcano e possibili considerazioni sui processi di degassamento attuali al cratere de La Fossa. CNR-GNV, Annu. Convention 8–10 June 1993, p. 264.

De Fino, M., La Volpe, L. and Piccarreta, G., 1991. Role of magma mixing during the recent activity of La Fossa di Vulcano (Aeolian Islands, Italy). J. Volcanol. Geotherm. Res., 48: 385–398.

Dellino, P., Frazzetta, G. and La Volpe, L., 1990. Wet surge deposits at La Fossa di Vulcano: depositional and eruptive mechanisms. J. Volcanol. Geotherm. Res., 43: 215–233.

Dobran, F., 1992. Nonequilibrium flow in volcanic conduits and application to the eruptions of Mt. St. Helens on May 18, 1980, and Vesuvius in AD 79. J. Volcanol. Geotherm. Res., 49: 285–311.

Dobran, F. and Papale, P., 1993. Magma-water interaction in closed systems and application to lava tunnels and volcanic conduits. J. Geophys. Res., 98: 14,041–14,058.

Dobran, F., Neri A. and Macedonio, G., 1993. Numerical simulation of collapsing volcanic columns. J. Geophys. Res., 98: 4231–4259.

Dolfi, D. and Trigila, R., 1978. The role of water in the 1944 Vesuvius eruption. Contrib. Mineral. Petrol., 67: 297–304.

Eggler, D.H., 1972. Water-saturated and undersaturated melting relations in a Paricutin andesite and an estimate of water content in the natural magma. Contrib. Mineral. Petrol., 34: 261–271.

Fabbri, A., Ghisetti, E. and Vezzani, L., 1980. The Peloritani-Calabria range and the Gioia Basin in the Calabrian Arc (Southern Italy): relationship between land and marine data. Geol. Rom., 19: 131–150.

Faraone, D., Silvano, A. and Verdiani, G., 1986. The monzogabbroic intrusion in the island of Vulcano, Aeolian Archipelago, Italy. Bull. Volcanol., 48: 299–307.

Ferrucci, F., Gaudiosi, G., Milano, G., Nercessian, A., Vilardo, G. and Luongo, G., 1991. Seismological exploration of Vulcano (Aeolian Islands, southern Tyrrhenian Sea): case history. Acta Vulcanol., 1: 143–152.

Frazzetta G., La Volpe, L. and Sheridan, M.F., 1983. Evolution of the Fossa Cone, Vulcano. J. Volcanol. Geotherm. Res., 17: 329–360.

Frazzetta, G., Gillot, P.Y., La Volpe, L. and Sheridan, M.F., 1984. Volcanic hazards at Fossa of Vulcano: data from the last 6,000 years. Bull. Volcanol. 47, 105–123.

Frazzetta, G. and La Volpe, L., 1987. Storia eruttiva dell'isola di Vulcano: stato di avanzamento della ricerca. Bol. G.N.V., pp. 361–372.

Gabbianelli, G., Romagnoli, C., Rossi, P.L., Calanchi, N. and Lucchini, F., 1991. Submarine morphology and tectonics of Vulcano (Aeolian Islands, Southeastern Tyrrhenian Sea). Acta Vulcanol., 1: 135–141.

Gasparini C., Iannaccone, G. and Scarpa, R., 1982. Seismotectonics of the Calabrian Arc. Tectonophysics, 84: 267–286.

Gioncada, A. and Sbrana, A., 1991. "La Fossa Caldera", Vulcano: inferences from deep drillings. Acta Vulcanol., 1: 115–125.

Gioncada, A. and Sbrana, A., 1993. Meccanismi eruttivi della eruzione del 1988–90 de La Fossa di Vulcano. CNR - Gruppo Nazionale per la Vulcanologia, Rapporto Su Vulcano, Giugno 1993.

Giordano, G. and Dobran, F., 1994. Computer simulations of the 2nd pyroclastic flow unit of Tuscolano Artemisio (Latium, Italy). J. Volcanol. Geotherm. Res., 61: 69–94.

Ghiorso, M.S., Carmichael, I.S.E., Rivers, M.L. and Sack, R.O., 1983. The Gibbs free energy of mixing of natural silicate liquids; an expanded regular solution approximation for the calculation of magmatic intensive variables. Contrib. Mineral. Petrol., 84: 107–145.

Ghisetti, F., 1979. Relazioni tra strutture e fasi trascorrenti e distensive lungo i sistemi Messina–Fiumefreddo, Tindari–Letojanni e Alia–Malvagna (Sicilia nord-orientale): uno studio microtettonico. Geol. Rom., 18: 23–58.

Keller, J., 1980. The island of Vulcano. Rend. Soc. Ital. Mineral. Petrol., 36: 369–414.

Kieffer, S.W. and Sturtevant, B., 1984. Laboratory studies of volcanic jets. J. Geophys. Res., 89: 8253–8268.

Kuntz, M.A., Rowley, P.D., Macleod, N.S., Reynolds, R.L., McBroome, L.A., Kaplan, A.M. and Lidke, D.J., 1981. Petrography and particle-size distribution of pyroclastic-flow, ash-cloud and surge deposits. U.S. Geol. Surv., Prof. Pap., 1250: 525–539.

Lange, R.A. and Carmichael, I.S.E., 1987. Densities of Na_2O-K_2O-CaO-MgO-FeO-Fe_2O_3-Al_2O_3-TiO_2-SiO_2 liquids: New measurements and derived partial molar properties. Geochim. Cosmochim. Acta, 51: 2931–2946.

Martini, M., Piccardi, G. and Cellini Legittimo, P., 1980. Geochemical surveillance of active volcanoes: data on the fumaroles of Vulcano (Aeolian Islands, Italy). Bull. Volcanol., 43: 255–263.

Mazor, E., Cioni, R., Corazza, E., Fratta, M., Magro, G., Matsuo, S., Hirabayashi, J., Shinohara, H., Martini, M., Piccardi, G. and Cellini Legittimo, P., 1988. Bull. Vulcanol., 50: 71–85.

McBirney, A.R., 1979. Volcanology, Freeman, Cooper & Co., San Francisco, CA., 397 pp.

Mercalli, G. and Silvestri, O., 1891. Le eruzioni dell'isola di Vulcano, incominciate il 3 Agosto 1888 e terminate il 22 Marzo 1890. Relazione scientifica. Ann. Uff. Cent. Meteor. Geodin., 10: 213–296.

Neri, A. and Dobran, F., 1994. Influence of eruption parameters on the dynamics and thermodynamics of collapsing volcanic columns. J. Geophys. Res., 99: 11,833–11,857.

Papale, P. and Dobran, F., 1993. Modeling of the ascent of magma during the plinian eruption of Vesuvius in AD 79. J. Volcanol. Geotherm. Res., 58: 101–132.

Papale, P. and Dobran, F. 1994. Magma flow along the volcanic conduit during the plinian and pyroclastic flow phases of the May 18, 1980 Mt. St. Helens eruption. J. Geophys. Res., 99: 4355–4373.

Shaw, H.R., 1972. Viscosities of magmatic silicate liquids: an empirical method of prediction. Am. J. Sci. 272: 870–893.

Sparks, R.S.J., 1978. The dynamics of bubble formation and growth in magmas, a review and analysis. J. Volcanol. Geotherm. Res., 3: 1–37.

Sparks, R.S.J. and Wilson. L., 1976. A model for the formation of ignimbrite by gravitational column collapse. J. Geol. Soc. London, 132: 441–451.

Valentine, G.A. and Wohletz, K.H., 1989. Numerical models of plinian eruption columns and pyroclastic flows. J. Geophys. Res., 94: 1867–1887.

Valentine, G.A., Wohletz, K.H. and Kieffer, S.W., 1991. Sources of unsteady column dynamics in pyroclastic flow eruptions. J. Geophys. Res., 96: 21887–21892.

Wilson, L. and Head III, J.W., 1981. Ascent and eruption of basaltic magma on the earth and moon. J. Geophys. Res., 86: 2971–3001.

Wilson, L., Sparks, R.S.J. and Walker, G.P.L., 1980. Explosive volcanic eruption — IV. The control of magma properties and conduit geometry on eruption column behavior. Geophys. J.R. Astron. Soc., 63: 117–148.

Wohletz, K.H., McGetchin, T.R., Sandford II, M.T. and Jones, E.M., 1984. Hydrodynamic aspects of caldera-forming eruptions: Numerical models. J. Geophys. Res., 89: 8269–8285.